

## Research Article

# Determination of Reference Ultrasound Parameters for Model and Hydrofluoroalkane Propellants Using High-Resolution Ultrasonic Spectroscopy

Susan Hoe,<sup>1</sup> Paul M. Young,<sup>1</sup> Philippe Rogueda,<sup>2</sup> and Daniela Traini<sup>1,3</sup>

Received 10 September 2007; accepted 26 March 2008; published online 6 May 2008

**Abstract.** The aim of this research was to determine the reference ultrasonic velocity ( $v$ ) and attenuation coefficient ( $\alpha$ ) for 2H, 3H-perfluoropentane (HPFP), 1,1,1,2-tetrafluoroethane (HFA-134a) and 1,1,1,2,3,3,3-tetrafluoroethane (HFA-227) propellants, for the future purpose of characterising pressurised metered dose inhaler (pMDI) formulations using high-resolution ultrasonic spectroscopy (HRUS). Perfluoroheptane (PFH) was used as a reference material for HPFP. With its velocity and attenuation coefficient determined at 25 °C, HPFP was subsequently used as a reference for HFA-134a and HFA-227. It was found that there is a linear decline in ultrasonic velocity with an increase in temperature. As with HPFP, the ultrasonic velocity of HFA-134a and HFA-227 were successfully calculated at 25 °C. However, the difference in density and viscosity between reference and sample prevented accurate determination of reference attenuation coefficient for the hydrofluoroalkanes. With ultrasonic velocity alone, dispersion concentration and stability monitoring for experimental pMDI formulations is possible using HRUS. However, at this point in time measurement of particle size is not feasible.

**KEY WORDS:** aerosols; pMDIs; suspension formulation; ultrasonic spectroscopy.

## INTRODUCTION

There are few established methods for characterization of pressurized metered dose inhaler (pMDI) suspension formulations. The majority of the techniques used to analyze characteristics such as particle size and stability are “indirect”, e.g. light diffraction (1–5), light scattering (6,7), post-actuation studies (8–10) or the use of model propellant (11). Despite their low-tech nature, visual and manual sedimentation analytical methods are still widely employed (12–14). The most commonly utilized method, *laser diffraction*, is relatively inexpensive, fast, and reliable for measuring particle size distribution (PSD) of pressurized metered dose inhaler suspensions (10) in hydrofluoroalkane propellants (HFAs). However, the low boiling points and high vapor pressure of HFA propellants limits their analysis to a transparent sealed system after high-pressure filling, making *in situ* analysis awkward with existing techniques. To circumvent this problem, alternative model propellants such as 2H, 3H-perfluoropentane (HPFP) have been chosen to replace HFA propellants in experimental conditions on the basis of similarity in physicochemical properties, but with a higher boiling point and lower volatility, allowing characterization at room temperature (11). Unfortunately, Jones

*et al.* (3) has shown that upon aerosolization, the use of surrogate solvents will not produce a particle size distribution which is comparable to that of HFA formulations. High-Resolution Ultrasonic Spectroscopy (HRUS) is a technique that utilizes ultrasonic waves instead of electromagnetic waves and which is capable of operating in pressurized systems, presenting an option for *in situ* characterization of pMDI solutions and suspensions. Several advantages of HRUS have been proposed:

1. No dilution steps required. Optical techniques require concentrated dispersions to be diluted in order to achieve sufficient optical transparency and avoid multiple scattering (1). In comparison, ultrasonic waves can propagate through concentrated dispersions without such requirements, avoiding the potential destruction of delicate flocs and aggregates (15).
2. Relatively fast measurements. The ability to make quick measurements presents HRUS as an attractive option for online analysis, particularly for flowing systems (1,15). This is in line with the Process Analytical Technology (PAT) (16), actively pursued by the Food and Drug Administration to design and develop processes that can consistently ensure a predefined quality at the end of the manufacturing process.
3. Overcomes several limitations of acoustic spectroscopy. Extensive literature going back to the 1950s details the acoustical properties of many solids and liquids (15,17,18). However, the application of acoustic spectroscopy in chemistry, biotechnology, pharmaceutical and food industries is limited by its inadequate

<sup>1</sup> Advanced Drug Delivery Group, Faculty of Pharmacy, University of Sydney, Sydney, New South Wales 2006, Australia.

<sup>2</sup> Novartis Horsham Research Centre, Wimbleshurst Road, Horsham, West Sussex, RH12 5AB, UK.

<sup>3</sup> To whom correspondence should be addressed. (e-mail: danielat@pharm.usyd.edu.au)

**Table I.** Selected Peaks for Measurement in PFH (Reference Cell) and HPFP (Sample Cell)

Peak	Frequency (kHz)		Peak number	
	PFH	HPFP	PFH	HPFP
A	7,716	8,535	166	166
B	7,948	8,791	171	171
C	7,995	8,843	172	172
D	8,087	8,945	174	174
E	8,225	9,048	177	177
F	8,365	9,201	180	180
G	8,457	9,304	182	182

resolution and large sample volumes (1,19–21). HRUS, as its name suggests, can achieve very high resolution (0.2 mm/s for ultrasonic velocity), and can analyse small sample volumes (down to 1 ml) (19,21).

## Theoretical Background

### Ultrasonic Spectroscopy Apparatus

The basic structure of any ultrasonic spectroscopy apparatus involves transducers which propagate ('transmitter') and collect ('receiver') an ultrasound wave through a sample. The wave is then converted into a digital signal, and analysed by the accompanying software. The HRUS bases its operation on the theory of wave resonance. One transducer behaves as both transmitter and receiver. A propagated ultrasonic wave is reflected back to the transducer, resulting in regions of constructive and destructive interference within the received wave.

### Ultrasonic Spectroscopy Parameters

The analysis of an ultrasonic wave is primarily concerned with three parameters: *ultrasonic velocity*, *attenuation* and *attenuation coefficient*.

*Ultrasonic Velocity (v)*. This parameter generally reflects the elastic nature of the liquid sample (16). It is inversely proportional to the density ( $\rho$ ) and adiabatic compressibility ( $\kappa$ ) of the liquid. Compressibility is easily influenced by the

structure and intermolecular interactions of the medium. Velocity is also highly sensitive to temperature, but relatively insensitive to changes in wave frequency (15).

*Attenuation*. The level of absorption experienced by a wave as it is propagated through the sample determines this parameter. Wave energy is transformed into translational energy during propagation, which may then be transformed further into other forms of energy, before thermal relaxation of the system. The time taken to complete this process creates a phase lag, thus reducing wave amplitude (18,22). Relaxation processes are believed to be a main contributor to ultrasound absorption in pure liquids (2), while scattering is a greater factor in dispersions.

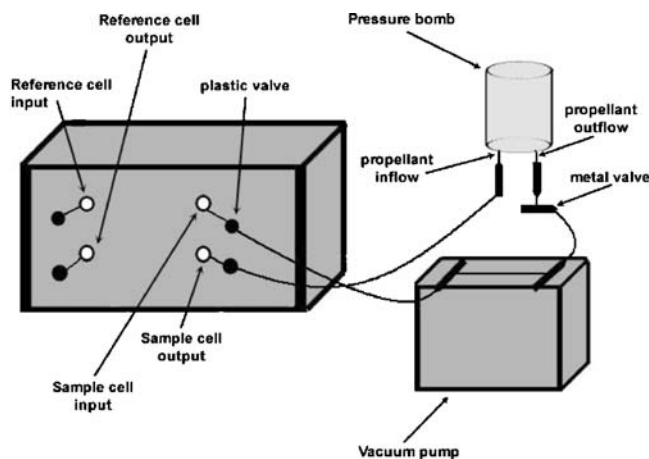
*Attenuation Coefficient ( $\alpha$ )*. The attenuation coefficient ( $\alpha$ ) normalizes the attenuation with the square of wave frequency (in hertz). The attenuation coefficient is expressed in units of  $s^2/m$ .

### Applications of HRUS Parameters

HRUS employs a mathematical model consisting of wave equations for sound propagation in suspensions, which relate attenuation to particle size. The equation is solved for one wave frequency, provided the mechanical and thermodynamic properties of the continuous and dispersed phases are known. HRUS utilises broadband pulses, so that the average particle

**Table II.** Temperature Ramp Protocol for PFH and HPFP

Stage	Initial temperature (°C)	End temperature (°C)	Duration of stage (h)
1	20	10	2
2	10	10	2
3	10	15	1
4	15	15	2
5	15	20	1
6	20	20	2
7	20	25	1
8	25	25	2
9	25	30	1
10	30	30	2

**Fig. 1.** Schematic of the HRUS apparatus connected to the propellant-filled pressure bomb, via a diaphragm pneumatic pump

**Table III.** Selected Peaks for Measurement in Pure HPFP (Reference Cell) and HFA-134a (Sample Cell)

Peak	Frequency (kHz)		Peak number	
	HPFP	HFA-134a	HPFP	HFA-134a
A	5,799	4,889	116	116
B	5,549	4,762	111	111
C	6,395	5,482	129	129
D	7,352	6,243	148	148
E	7,650	6,452	153	153
F	8,846	7,516	177	177
G	8,945	7,600	179	179

size is ascertained from the assemblage of solutions which arise from the entire set of wave equations for the frequency range. A similar wave equation relates velocity and wave frequency to dispersed phase concentration (1,23). Rogueda *et al* (24) have used HRUS to monitor average particle size and concentration of HFA suspensions in commercial pMDIs, essentially quantifying the phenomenon of phase separation. However, determination of reference parameters for propellants is a necessary step towards theoretical modelling of pMDI solutions and suspensions, if the application of HRUS is to be extended to on-line measurements and analysis of experimental pMDI formulations.

#### Ultrasonic Parameters Measurement

HRUS software measures a sample's parameters relative to those of a reference media (whose parameters are already known) in order to infer an absolute value for sample parameters, where sample and reference are contained in separate cells. While sound waves consist of regions of compression and rarefaction, the software graphically displays these waves as peaks, reflecting wave amplitude and bandwidth. In order to track the changes in a wave when comparing its frequency in the reference media, to its frequency in the sample, the same peak must be detected in both media. To facilitate this process, every peak is assigned an integer called a *peak number*, ascending with frequency. By measuring the shift in a particular peak's frequency from reference to sample, the relative change in ultrasonic velocity can be determined. As the actual velocity in the reference media is known, the absolute ultrasonic velocity in the sample can be calculated. Similarly, by measuring the change in peak bandwidth, the relative attenuation coefficient of the sample

may be determined, leading to a calculation of absolute attenuation coefficient. The selection of an appropriate peak to follow may be as important as the measurement itself.

Published research using HRUS for bench testing of commercial pMDIs has been carried out at 25 °C. For consistency, the aim of this project was to determine the ultrasonic reference parameters  $\alpha$  and  $\nu$  at 25 °C, for the model propellant HPFP, and the hydrofluoroalkane propellants HFA-134a and HFA-227. Ideally these parameters will form the basis for a bank of ultrasound data, in which reference parameters for common combinations of propellant, excipients, and actives are recorded to achieve a better understanding of the contributions of each component to the physicochemical properties of the formulation as a whole. HRUS could also potentially act as an on-line process analyser for pMDI manufacturing with this information. A key requirement of an appropriate reference media to use for HR-US measurements is an acceptable similarity to the sample in physicochemical characteristics, to assist the software in tracking the same peak from reference to sample. For this reason, perfluoroheptane (PFH) was selected as the reference media for HPFP, which would itself become a reference media for the hydrofluoroalkane propellants (15).

#### MATERIALS AND METHODS

Perfluoroheptane (PFH) and 2H, 3H-perfluoroheptane (HPFP) were purchased from Fluorochem Ltd (UK). Aluminium Oxide (basic and acidic) was purchased from Fluka (UK). HFA-134a was purchased from INEOS Fluor Ltd (UK) and HFA-227 from Solvay Fluor (Germany). Solvents were supplied by BDH (Poole, UK) and were of analytical grade. The equipment used for the ultrasonic spectroscopy

**Table IV.** Selected Peaks for Measurement in Pure HPFP (Reference Cell) and HFA-227 (Sample Cell)

Peak	Frequency (kHz)		Peak number	
	HPFP	HFA-227	HPFP	HFA-227
A	1,803	2,337	35	35
B	1,704	2,406	34	34
C	2,499	2,613	50	50
D	3,442	4,841	70	70
E	4,002	5,637	81	81
F	4,151	5,776	83	83
G	4,301	6,009	86	86

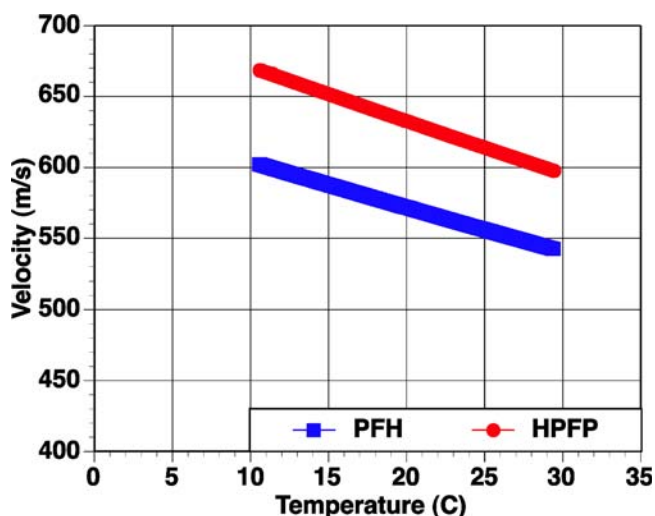


Fig. 2. Effect of temperature ( $^{\circ}\text{C}$ ) of the selected peaks on ultrasonic velocity (m/s) for PFH and HPFP

analysis was the HR-US S1 Sedimentation Analyser (Ultrasonic Scientific Ltd, Ireland) equipped with computer software (HR-US s1 Build 4.50.29.22) Ultrasonic Sedimentation Analyser software (Ultrasonic Scientific Ltd, Ireland). The Haake Phoenix II C25P water bath (Thermo Electron Corporation, Germany) was used for temperature control of the reference and sample cells.

#### Model Propellant Purification

Commercially available PFH and HPFP were purified before use. Cellulose nitrate filter membranes (0.2  $\mu\text{m}$  pore size, Sigma-Aldrich Company Ltd, UK) were loaded into disposable vacuum filter units (Nalgene, USA) and were used for the purification of PFH and HPFP. The purity of both PFH and HPFP was in excess of 99.9%, with moisture content less than 9 ppm. Further purification of both model propellants was achieved by filtering and purifying with chromatographic grade acidic and basic alumina (Fluka, Gillingham, UK). This treatment was necessary to remove impurities in the organic liquid, which may otherwise directly influence measurements (25). Approximately 200 g acidic aluminium oxide was added to a filter unit, followed by vacuum filtration for each 2 L of model propellant. The container was sealed and agitated by a Turbula Mixer (Glen Creston Limited, UK) for 45 min. Two hundred grams of basic aluminium oxide were placed in a new filter unit, and the agitated mixture was filtered, removing all acidic aluminium oxide. The resultant model propellants/basic aluminium oxide mixture was also agitated in the Turbula Mixer for 45 min, before removal of all basic aluminium oxide from the mixture by filtration. The supernatant was then sonicated using the Ultrawave Sonicator DP200-00 (Ultrawave Limited, UK) for 5 min to remove any traces of dissolved gas.

#### Determination of HPFP Ultrasonic Parameters

PFH was chosen for deriving ultrasonic parameters for HPFP, as its ultrasonic parameters,  $\alpha$  and  $v$ , were already known, although only at 20  $^{\circ}\text{C}$  (Private Communication, Ultrasonic Scientific Ltd, Ireland). Consequently, initial tests carried

out with PFH as reference and HPFP as sample had to be operated at 20  $^{\circ}\text{C}$  to achieve accurate relative measurements. As the aim was to use HPFP as a reference material to determine ultrasonic parameters for the HFA propellants at 25  $^{\circ}\text{C}$ , it was necessary to run a temperature ramp and observe subsequent changes to velocity and attenuation, in order to discover reference parameters for HPFP at 25  $^{\circ}\text{C}$ . The reference ultrasonic parameters for PFH at 20  $^{\circ}\text{C}$  were:  $v=572.2$  m/s,  $\alpha=(3.9\pm 0.3)\times 10^{-13}$  s<sup>2</sup>/m,  $\rho=1,620$  kg/m<sup>3</sup> and were used for analytical calculation.

A water bath was set to 20  $^{\circ}\text{C}$  and left to equilibrate for 10 min to ensure the HRUS cells reached equilibrium. The cells were rinsed with MilliQ water, then ethanol, before drying with pressurised nitrogen gas. PFH was slowly filled into the reference cell using a 20 ml plastic syringe. Care was taken in ensuring no air bubbles were present in the cell. This procedure was repeated for HPFP in the sample cell. Both liquids were left to equilibrate at 20  $^{\circ}\text{C}$  for 5 min. A frequency scan was carried out from 2,000 to 10,000 kHz for both PFH and HPFP to identify appropriate peaks. Peak numbers were assigned to the selected peaks in PFH, and used to detect their respective position in HPFP (Table I). The change in peak frequency and bandwidth from PFH to HPFP was measured for each peak over a temperature ramp, starting at 20  $^{\circ}\text{C}$ , before declining to 10  $^{\circ}\text{C}$  and then increasing to 30  $^{\circ}\text{C}$  (Table II). This step enabled calculation of attenuation and velocity in the liquids at 10, 15, 20, 25 and 30  $^{\circ}\text{C}$ . Regression equations were applied to ultrasound parameter *versus* temperature plots for PFH and HPFP, from which the reference parameters for HPFP at 25  $^{\circ}\text{C}$  were estimated.

#### Determination of HFA-134a and HFA-227 Ultrasonic Parameters at 25 $^{\circ}\text{C}$

Reference parameters for HPFP at 25  $^{\circ}\text{C}$  were derived as mentioned above. A summary of all findings can be found in Table V. HFA-134a propellant (impurities less than 1 ppm w/w,

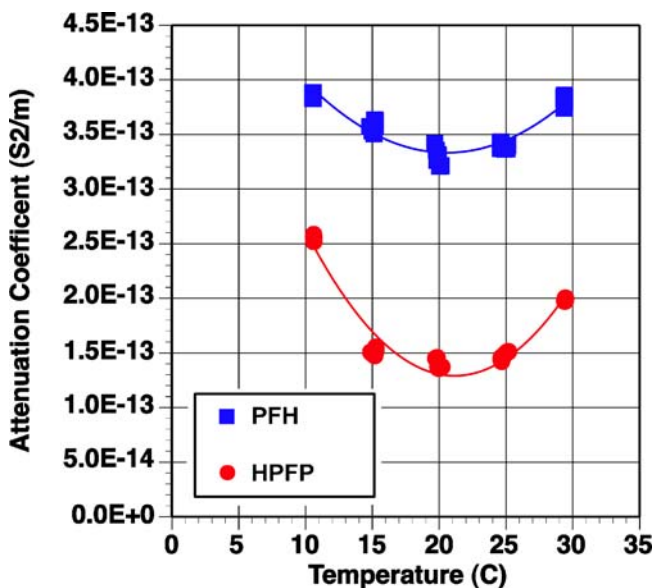


Fig. 3. Effect of temperature ( $^{\circ}\text{C}$ ) on attenuation coefficient (s<sup>2</sup>/m) for PFH and HPFP

**Table V.** Summary of All Media Parameters Calculated for PFH, HPFP, HFA-134a and HFA-227

	PFH (20 °C)	HPFP (20 °C)	HPFP (25 °C)	HFA-134a (25 °C)	HFA-227 (25 °C)
Velocity (m/s)	572.2 ( $\pm 0.0$ )	633.0 ( $\pm 0.0$ )	614.0 ( $\pm 0.4$ )	521.1 ( $\pm 1.7$ )	856.0 ( $\pm 4.3$ )
Attenuation coefficient ( $\text{s}^2/\text{m}$ )	$3.9 \times 10^{-13}$ ( $\pm 1.7 \times 10^{-15}$ )	$1.37 \times 10^{-13}$ ( $\pm 2.6 \times 10^{-16}$ )	$1.45 \times 10^{-13}$ ( $\pm 1.88 \times 10^{-15}$ )	N/A	N/A
Temperature velocity increment ( $\text{m s}^{-1} \text{ } ^\circ\text{C}^{-1}$ )	-3.2	-3.8	-3.8	-5.0	-8.9

( $\pm$ SD=standard deviation,  $n=3$ )

from the certificate of analysis) was cold-filled into an in-house pressure bomb, up to approximately two-thirds the height of the container, before being sealed and placed in a water bath to allow temperature equilibration.

As with the above experiment, pure HPFP was filled into the reference cell. The HFA-134a pressure bomb output valve was connected to a liquid pump (KNF Neuberger, Switzerland), which was in turn connected to the HRUS sample cell input; the sample cell output was connected directly to the pressure bomb input valve (Fig. 1). The sample cell was filled with propellant and both HPFP, and the propellants were left for 5 min to equilibrate at 25 °C. A frequency scan was carried out for the reference and sample liquids, ranging from 2,000 to 10,000 kHz. As HFA-134a appeared to have narrower regions of usable peaks than HPFP, the peaks were selected from the HFA-134a scan, and peak numbers were assigned to them in order to detect their positions in HPFP (Table III). The change in peak frequency and bandwidth from HPFP to HFA-134a was measured for each peak over 60 min, enabling calculation of attenuation and velocity in these liquids. The above procedure was repeated for HFA-227 (impurities less than 1 ppm  $w/w$ , from the certificate of analysis; Table IV).

## RESULTS AND DISCUSSION

### Determination of HPFP Ultrasonic Parameters

At 20 °C, the ultrasonic velocity of HPFP was found to be  $633.02 \pm 0.05$  m/s. The results of the temperature ramp of the selected peaks are presented in Fig. 2. A good linear correlation was found between temperature and ultrasonic velocity for both PFH and HPFP. Regression coefficients were  $R^2=0.9999$  for both PFH and HPFP. Using linear regression, the ultrasonic velocity of HPFP at 25 °C was calculated to be 614.02 m/s, with a temperature velocity increment of  $-3.77 \text{ m s}^{-1} \text{ } ^\circ\text{C}^{-1}$ . This decline in ultrasonic velocity is consistent with temperature ramps conducted on pure hydrocarbons media, indicating that the compressibility of HPFP increases with temperature, resulting in a decrease in ultrasonic velocity (5).

The relationship between attenuation coefficient and temperature is harder to explain (Fig. 3). At higher temperatures, sound absorption in these propellants may be mostly through translational energy coupled to thermal relaxation. An increase in temperature increases molecular collisions, and hence there is a greater wave energy loss, leading to

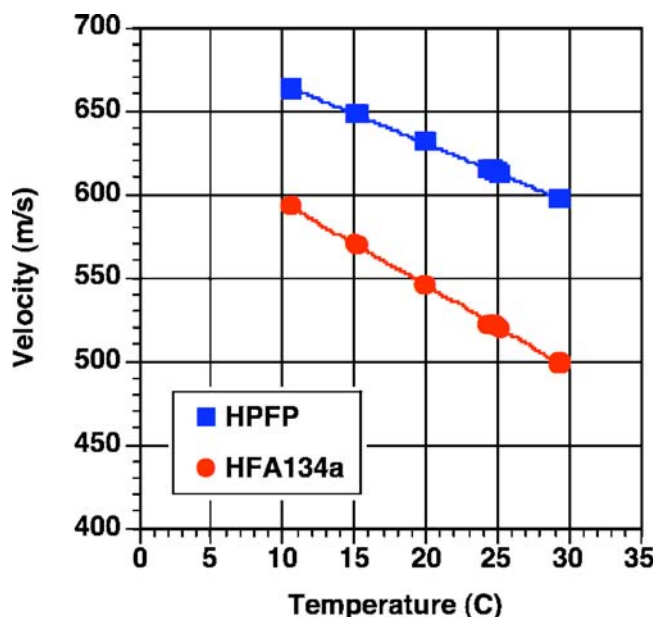


**Fig. 4.** Effect of temperature (°C) on ultrasonic velocity of HPFP and HFA-134a

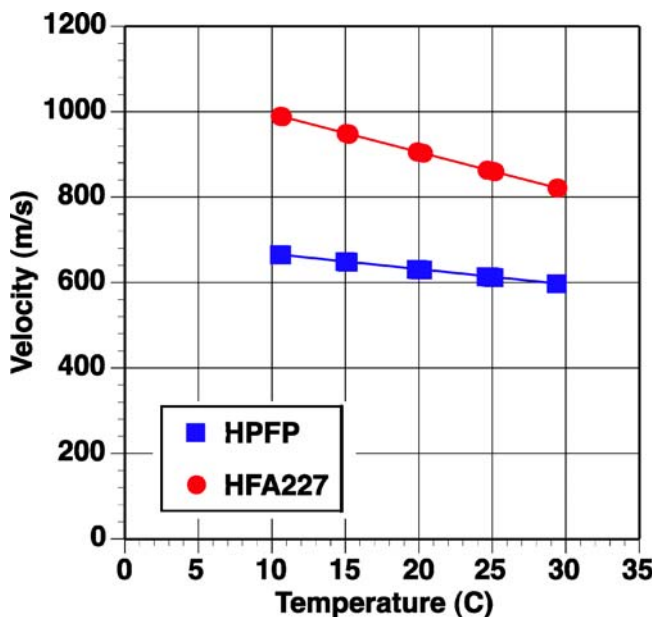


**Fig. 5.** Effect of temperature (°C) on ultrasonic velocity (m/s) of HPFP and HFA-227

larger attenuation. At lower temperatures, the dominant process of sound absorption is via translational energy coupled to shear and structural relaxation, related to shear and volume viscosity. It is understood that the propagated wave will disrupt a weak liquid lattice structure, which requires time to relax. Consequently the phase lag in the return of energy to the wave results in attenuation. As temperature decreases, viscosity of these liquids increase, and attenuation is also expected to increase (11,18). The trough observed at around 20 °C in Fig. 3 indicates a temperature range where there is minimal wave energy loss from the two processes described above.

The following second order polynomial regression equations (Eqs. 1 and 2) were used to describe the relationship between attenuation coefficient and temperature:

$$\text{PFH : } y = 5.8278651 \times 10^{-16}x^2 - 2.3978088 \times 10^{-14}x + 5.7985744 \times 10^{-13} \quad (1)$$

$$\text{HPFP : } y = 1.0666072 \times 10^{-15}x^2 - 4.5133832 \times 10^{-14}x + 6.0646189 \times 10^{-13} \quad (2)$$

Regression coefficients were:  $R^2=0.9310$  and  $R^2=0.9679$ , for PFP and HPFP, respectively.

Using Eq. 2, the attenuation coefficient of HPFP at 25 °C was estimated to be  $1.45 \times 10^{-13}$  s<sup>2</sup>/m. With the  $\nu$  and  $\alpha$  parameters determined at 25 °C (Table V), HPFP was then used as the reference media for the hydrofluoroalkane propellants at this temperature.

#### Determination of HFA-134a and HFA-227 Ultrasonic Parameters at 25 °C

The average ultrasonic velocity for HFA-134a at 25 °C, using HPFP as the reference media, was  $521.1 \pm 1.7$  m/s. This is lower than the ultrasonic velocity in HPFP (614.02 m/s). Since the density of HFA-134a at 25 °C ( $1,208$  kg/m<sup>3</sup>) is lower than that of HPFP ( $1,583$  kg/m<sup>3</sup>), this observation may be the consequence of greater intermolecular interaction (specifically London forces) between HPFP molecules, resulting in less compressibility and thus greater velocity than HFA-134a. The results of the temperature ramp of the selected peaks are presented in Fig. 4. There is a very good linear correlation ( $R^2=1$ ) between temperature and ultrasonic velocity. From this plot the following linear regression equation for HFA-134a was derived:

$$y = -4.9758x + 644.82 \quad (3)$$

From Eq. 3, the temperature velocity increment for HFA-134a was determined to be  $-4.97$  m s<sup>-1</sup> °C<sup>-1</sup>.

As with HFA-134a, the ultrasonic velocity for HFA-227 was calculated as an average of velocities and attenuation coefficients for the selected peaks measured over 60 min. The average ultrasonic velocity for HFA-227 at 25 °C was  $859.9 \pm 4.3$  m/s. However, unlike HFA-134a, this is higher than ultrasonic velocity in HPFP, indicating HFA-227 has lower compressibility compared to HPFP.

The results of the temperature ramp for HFA-227 are presented in Fig. 5. There is a very good correlation between temperature and ultrasonic velocity. The following linear regression equation for HFA-227 was derived:

$$y = -8.9222x + 1083.7 \quad (R^2 = 1) \quad (4)$$

As can be observed from Eq. 4, the temperature velocity increment for HFA-227 is  $-8.9$  m s<sup>-1</sup> °C<sup>-1</sup>.

HPFP is considered to be a model HFA propellant on the basis that it is a commercially available material with physicochemical properties similar to that of the hydrofluoroalkane propellants, but existing as a liquid at room temperature, making it ideal for modelling pMDI suspensions in standard laboratory conditions. To facilitate peak tracking, it is preferred to select sample and reference pairs whose attenuation coefficients are as close as possible. For this reason, HPFP was deemed the most suitable reference material for HFAs. However, HPFP has approximately double the viscosity of the hydrofluoroalkanes, and the density of HPFP is  $1.583$  g/cm<sup>3</sup>, which is larger than HFA-227 ( $1.388$  g/cm<sup>3</sup>) and HFA-134a ( $1.208$  g/cm<sup>3</sup>) (11). It is postulated that despite the general similarity between HPFP and the HFAs, there may have been too great a difference in attenuation coefficient, due to the disparity in viscosity and density. This hindered the finding of ideal peaks to track from reference to sample, and prevented accurate determination of the attenuation coefficient at 25 °C for both HFA-134a and HFA-227.

#### CONCLUSIONS

In this study, the ultrasonic velocity was successfully determined for 2H, 3H-perfluoropentane (HPFP), HFA-134a and HFA-227 at 25 °C. With this knowledge, it is possible to analyse dispersion concentration, and monitor stability of pMDI formulations, as velocity is an indicator of changes to the compressibility of the continuous phase. However, the lack of a definite attenuation coefficient for these propellants delays the possibility of measuring the average particle size of experimental pMDI formulations using HRUS.

#### ACKNOWLEDGEMENTS

The authors gratefully acknowledge the financial support from the Faculty of Pharmacy at the University of Sydney (Australia) and AstraZeneca R&D Loughborough (UK).

#### REFERENCES

1. F. Alba, G. M. Crawley, J. Fatkin, D. M. J. Higgs, and P. G. Kippax. Acoustic spectroscopy as a technique for the particle sizing of high concentration colloids, emulsions and suspensions. *Colloids Surf A Physicochem Eng Asp.* **153**:495–502 (1999).
2. Z. Ma, H. G. Merkus, J. G. A. E. Smetde, C. Heffels, and B. Scarlett. New developments in particle characterization by laser diffraction: size and shape. *Powder Technol.* **111**:66–78 (2000).
3. S. A. Jones, G. P. Martin, and M. B. Brown. High-pressure aerosol suspensions—A novel laser diffraction particle sizing system for hydrofluoroalkane pressurised metered dose inhalers. *Int J Pharm.* **302**:154–165 (2005).

4. J. Ziegler, and H. Wachtel. Comparison of cascade impaction and laser diffraction for particle size distribution measurements. *J Aerosol Sci.* **18**:311–324 (2005).
5. W. T. J. Kwong, S. L. Ho, and A. L. Coates. Comparison of nebulized particle size distribution with Malvern laser diffraction analyzer versus Andersen cascade impactor and low-flow Marple personal cascade impactor. *J Aerosol Med.* **13**:303–314 (2000).
6. C. Lemarchand, P. Couveur, C. Vauthier, D. Constantini, and R. Gref. Study of emulsion stabilization by graft copolymers using the optical analyzer Turbiscan. *Int J Pharm.* **254**:77–82 (2003).
7. O. Mengual, G. Meunier, I. Cayre, K. Puech, and P. Snabre. Characterisation of instability of concentrated dispersions by a new optical analyser: the TURBISCAN MA 1000. *Colloids Surf A Physicochem. Eng. Asp.* **152**:111–123 (1999).
8. R. Ashayer, P. F. Luckham, S. Manimaaran, and P. Rogueda. Investigation of the molecular interactions in a pMDI formulation by atomic force microscopy. *Eur. J. Pharm. Sci.* **21**:533–543 (2004).
9. H. D. Smyth. The influence of formulation variables on the performance of alternative propellant-driven metered dose inhalers. *Adv. Drug. Deliv. Rev.* **55**:807–828 (2003).
10. S. A. Jones, G. P. Martin, and M. B. Brown. Manipulation of beclomethasone-hydrofluoroalkane interactions using biocompatible macromolecules. *J. Pharm. Sci.* **95**:1060–1074 (2006).
11. P. G. Rogueda. HPFP, a Model Propellant for pMDIs. *Drug Dev. Ind. Pharm.* **29**:39–49 (2003).
12. R. O. Williams 3rd, M. A. Repka, and M. K. Barron. Application of co-grinding to formulate a model pMDI suspension. *Eur. J. Pharm. Biopharm.* **48**:131–140 (1999).
13. Y. Michael, M. J. Snowden, B. Z. Chowdhry, I. C. Ashurst, C. J. Davies-Cutting, and T. Riley. Characterisation of the aggregation behaviour in a salmeterol and fluticasone propionate inhalation aerosol system. *Int. J. Pharm.* **221**:165–174 (2001).
14. A. Brindley. The chlorofluorocarbon to hydrofluoroalkane transition: the effect on pressurised metered dose inhaler stability. *J. Allergy Clin. Immunol.* **104**:S211–226 (1999).
15. A. S. Dukhin, and P. J. Goetz. *Ultrasound for characterising colloids—Particle sizing, Zeta Potential, Rheology*, Elsevier Science B.V., Amsterdam, 2002.
16. U.S. Department of Health and Human Services, Food and Drug Administration, Center for Drug Evaluation and Research (CDER), Center for Veterinary Medicine (CVM), Office of Regulatory Affairs (ORA). Guidance for Industry PAT—A Framework for Innovative Pharmaceutical Development, Manufacturing, and Quality Assurance <http://www.fda.gov/Cder/guidance/6419fnl.pdf>.
17. V. A. del Grosso and C. W. Mader. Speed of Sound in Pure Water. *J. Acoust. Soc. Am.* **52**:1442–1972 (1972).
18. T. A. Litovitz. Ultrasonic spectroscopy in liquids. *J. Acoust. Soc. Am.* **11**:681–691 (1959).
19. V. A. Buckin, E. Kudryashov, and B. O'Driscoll. High-resolution ultrasonic spectroscopy for material analysis. *Am. Lab.* **34**:28, 31–32 (2002).
20. J. R. Allegra, and S. A. Hawley. Attenuation of sound in suspensions and emulsions: Theory and experiments. *J. Acoust. Soc. Am.* **51**:1545–1564 (1971).
21. L. Lehmann and V. Buckin. Determination of the heat stability profiles of concentrated milk and milk ingredients using high resolution ultrasonic spectroscopy. *J. Dairy. Sci.* **88**:3121–3129 (2005).
22. V. A. Buckin, and C. Smyth. High-resolution ultrasonic resonator measurements for analysis of liquids. *Semin. Food Anal.* **4**:89–105 (1999).
23. U. Riebel, and F. Löffler. The fundamentals of particle size analysis by means of ultrasonic spectrometry. *Part Part Syst. Charact.* **6**:135–143 (1989).
24. P. G. Rogueda, V. Buckin, and E. Kudryashov. Size and concentration monitoring of hfa suspensions. *Respiratory Drug Delivery X*. April 23–27, 2006; Boca Raton, FL
25. A. Goebel, and K. Lunkenheimer. Interfacial tension of the water/n-alkane interface. *Langmuir.* **13**:369–372 (1997).